Beyond geolocating: Constraining higher dimensional operators in $H \to 4\ell$ with off-shell production and more

James S. Gainer,[1] Joseph Lykken,[2] Konstantin T. Matchev,[1] Stephen Mrenna,[3] and Myeonghun Park[4]

[1]*Physics Department, University of Florida, Gainesville, Florida 32611, USA*
[2]*Theoretical Physics Department, Fermilab, Batavia, Illinois 60510, USA*
[3]*SSE Group, Computing Division, Fermilab, Batavia, Illinois 60510, USA*
[4]*Kavli IPMU (WPI), The University of Tokyo, Kashiwa 277-8583, Japan*
(Received 28 March 2014; published 11 February 2015)

We extend the study of Higgs boson couplings in the "golden" $gg \to H \to ZZ^* \to 4\ell$ channel in two important respects. First, we demonstrate the importance of off-shell Higgs boson production ($gg \to H^* \to ZZ \to 4\ell$) in determining which operators contribute to the HZZ vertex. Second, we include the five operators of lowest nontrivial dimension, including the $Z_\mu Z^\mu \Box H$ and $H Z_\mu \Box Z^\mu$ operators that are often neglected. We point out that the former operator can be severely constrained by the measurement of the off-shell $H^* \to ZZ$ rate and/or unitarity considerations. We provide analytic expressions for the off-peak cross sections in the presence of these five operators. On shell, the $Z_\mu Z^\mu \Box H$ operator is indistinguishable from its Standard Model counterpart $H Z_\mu Z^\mu$, while the $H Z_\mu \Box Z^\mu$ operator can be probed, in particular, by the Z^* invariant mass distribution.

I. INTRODUCTION

Now that a Standard Model (SM)-like Higgs boson has been discovered at the Large Hadron Collider (LHC) [1,2], it is critical to measure its couplings. The sensitivity of the $H \to ZZ^* \to 4\ell$ to the couplings of the putative Higgs boson to Z bosons is well established theoretically [3–58]; measurements of this channel have indeed been performed by the experimental collaborations [59–66].

Recently, the importance of the off-shell cross section ($M_{4\ell} \gg 125$ GeV) for measuring the full width of the Higgs boson has been demonstrated [30,49,56,67–69]. We point out that the off-shell cross section in this channel is also useful for constraining anomalous HZZ couplings, since these anomalous operators are of a higher dimension and can enhance the production cross section at large values of the invariant mass. Previous studies of Higgs boson couplings at the LHC (see, e.g. Ref. [70] and references therein) have focused on three specific operators, one of mass dimension three and two of mass dimension five. Here we also study two additional dimension-five operators that are suppressed on shell [45] (see also Refs. [71–76]).

In Sec. II, we discuss parametrizations of the XZZ couplings (we consider an arbitrary scalar, X, in our discussions). Five independent operators (or equivalently, five independent Lorentz structures in the amplitude) should be considered. The measurement of the couplings of these five operators is the cornerstone of the future LHC physics program and will proceed in several stages:

(1) The measurement of the overall signal rate in the four-lepton channel from an on-shell Higgs boson provides an important constraint on these five operators, effectively reducing the parameter space

by one dimension [45]. This "geolocating" procedure is reviewed and extended to five degrees of freedom in Sec. III.

(2) The measurement of the Higgs boson contribution to the ZZ continuum at high invariant masses provides a second, independent constraint that is the subject of Sec. IV.

(3) Finally, precision measurements of decay kinematics on the Higgs boson peak provide additional information on the tensor structure of the XZZ couplings, as discussed in Sec. V.

The goal of this paper is to consider the most general XZZ couplings involving operators up to mass dimension five *without theoretical prejudice*. This is precisely the approach taken in four-lepton analyses by the ATLAS and CMS collaborations [59–66]—our contribution here is to point out the existence of additional operators and identify their phenomenological consequences. In doing so, we shall steer clear of any theory bias. For example, we shall not assume any particular representation of the "Higgs" resonance, nor shall we assume that $SU(2) \times U(1)$ gauge symmetry is necessarily preserved in the full effective field theory. (After all, electroweak symmetry is at least apparently broken.) We shall not make any assumptions about the complete set of operators that would be generated; in particular we are not concerned with $XZ\gamma$, $X\gamma\gamma$, or XWW operators.[1] In this sense, our paper is complementary to many other studies in the literature, which have made some

---

[1]Of course, if one has a complete set of operators, one could also constrain their coefficients from precision electroweak data along the lines of Refs. [77–91].

or all of these assumptions [41,71,74,92–125]. We discuss possible unitarity violation in detail and give guidance on how to deal with this issue when using our parametrization of *XZZ* couplings. We also point out the importance of anomalous couplings when studying off-shell four-lepton events, though we leave a precise estimation of the experimental sensitivity to these effects (which would have to include interference with continuum $gg \to ZZ$ production) to future studies.

II. PARAMETRIZATION OF *XZZ* COUPLINGS

There are two obvious and equivalent approaches to describing the coupling of an arbitrary spin-zero scalar to two *Z* bosons:

(1) Introducing a general amplitude for $X \to Z_{\lambda_1} Z_{\lambda_2}$,[2] as is done, e.g. in Refs. [19,20,34], or

(2) Through the operators in an effective theory Lagrangian.

The correspondence between these two prescriptions is as follows:

$$i\epsilon_1^* \cdot \epsilon_2^* \Leftrightarrow -\frac{1}{2}XZ_\mu Z^\mu, \qquad (1)$$

$$i(p_1 \cdot p_2)(\epsilon_1^* \cdot \epsilon_2^*) \Leftrightarrow \frac{1}{2}X\partial_\mu Z_\nu \partial^\mu Z^\nu, \qquad (2)$$

$$i(p_1 \cdot \epsilon_2^*)(p_2 \cdot \epsilon_1^*) \Leftrightarrow \frac{1}{2}X\partial_\mu Z_\nu \partial^\nu Z^\mu, \qquad (3)$$

$$i\epsilon_{\mu\nu\rho\sigma}\epsilon_1^{*,\mu}\epsilon_2^{*,\nu}p_1^\rho p_2^\sigma \Leftrightarrow -\frac{1}{2}\epsilon_{\mu\nu\rho\sigma}\partial^\mu Z^\nu \partial^\rho Z^\sigma, \qquad (4)$$

$$i(p_1^2 + p_2^2)(\epsilon_1^* \cdot \epsilon_2^*) \Leftrightarrow XZ_\mu \Box Z^\mu, \qquad (5)$$

where $\epsilon_1^\mu = \epsilon^\mu(p_1)$ and $\epsilon_2^\mu = \epsilon^\mu(p_2)$ are gauge boson polarization vectors. The five operators (1)–(5) are dimension five or less.[3] These operators correspond to the five independent amplitude structures which have mass dimension two or less.

In either approach, there is the freedom to choose the most convenient set of operators as a basis for a particular application. Our basis is described below:

(1) The expression (1) is proportional to the tree-level SM Higgs boson coupling.[4] For convenience, we therefore define

$$\mathcal{O}_1 = -\frac{M_Z^2}{v}XZ_\mu Z^\mu, \qquad (6)$$

where v is the Higgs vacuum expectation value, 246 GeV; hence $\mathcal{O}_1$ is equal to the tree-level SM coupling.

(2) Of the five operators, only (4) is invariant under the gauge transformation $Z_\mu \to Z_\mu + \partial_\mu \chi$.[5] We therefore define

$$\mathcal{O}_3 = -\frac{1}{2v}XF_{\mu\nu}\tilde{F}^{\mu\nu} \qquad (7)$$

to be proportional to this expression, where $\tilde{F}_{\mu\nu} = \frac{1}{2}\epsilon_{\mu\nu\rho\sigma}F^{\rho\sigma}$ and $F_{\mu\nu} = \partial_\mu Z_\nu - \partial_\nu Z_\mu$.

(3) None of the remaining four operators in (1)–(5) are individually gauge invariant, but the difference of expressions (2) and (3) is. We therefore define $\mathcal{O}_2$ to be proportional to this difference:

$$\mathcal{O}_2 = -\frac{1}{2v}XF_{\mu\nu}F^{\mu\nu}. \qquad (8)$$

In Ref. [45], we presented a framework for measuring the couplings of the putative Higgs boson *X* to a pair of gauge bosons with a primary focus on the "golden" $X \to ZZ^* \to 4\ell$ channel. In that work, we considered in detail only $\mathcal{O}_1$, $\mathcal{O}_2$, and $\mathcal{O}_3$ and described how, after fixing the overall rate, the measurements of the coefficients of these operators corresponded to the "geolocation" of the Higgs boson couplings on a suitably defined sphere. In this work, we will explore the phenomenological consequences of performing such measurements in the full five-dimensional operator space, in particular considering operators which were mentioned, but ultimately neglected, in Ref. [45].

Before proceeding, we note that, in general, complex contributions to the form factors in the amplitude can be generated through loops involving light particles; schemes for measuring the coupling in such scenarios were discussed in Ref. [45]. However, such loop-induced contributions are expected to be small (see, e.g. Ref. [53]). All couplings are taken to be real in the analysis presented here.

To study the phenomenological consequences of the full five-dimensional operator space, we must first identify the two basis operators not space spanned by $\mathcal{O}_1$, $\mathcal{O}_2$, and $\mathcal{O}_3$. A convenient choice, for phenomenological reasons, is

---

[2]The *Z* bosons have arbitrary invariant masses. We will not assume any *Z* boson to be on shell, unless explicitly noted.

[3]If we assume that the overall constant contains one power of the vacuum expectation value, we must refer to, e.g. a dimension-five operator as a dimension-six operator.

[4]Electroweak corrections to the SM $H \to 4\ell$ process are discussed, for example, in Refs. [126,127].

[5]Invariance under the full set of $SU(2) \times U(1)$ gauge transformations depends on the coefficients of the corresponding operators in $X \to WW$, $X \to Z\gamma$, and $X \to \gamma\gamma$. As we are only considering $X \to ZZ$ channels, we will use the term "gauge invariant" to mean invariant under $Z_\mu \to Z_\mu + \partial_\mu \chi$.

$$\mathcal{O}_5 = \frac{2}{v} X Z_\mu \Box Z^\mu, \tag{9}$$

which is proportional to the operator in expression (5). For the final basis operator, one choice is

$$\mathcal{O}_4 = \frac{M_Z^2}{M_X^2 v} \Box X Z_\mu Z^\mu, \tag{10}$$

where M_X is the mass of the putative Higgs boson (≈ 125 GeV). This operator is equivalent to the operators in expressions (2) and (5) after using integration by parts. Specifically,

$$\mathcal{O}_4 \Leftrightarrow \frac{M_Z^2}{M_X^2 v} X(\partial_\mu Z_\nu \partial^\mu Z^\nu + Z_\mu \Box Z^\mu), \tag{11}$$

which can be seen directly by considering the corresponding amplitudes. As an alternative to $\mathcal{O}_4$, we will also consider an operator which is proportional to the sum of the operators in expressions (2) and (3) and hence is orthogonal to $\mathcal{O}_2$. We define this operator as

$$\mathcal{O}_6 = \frac{1}{v} X(\partial_\mu Z_\nu \partial^\nu Z^\mu + \partial_\mu Z_\nu \partial^\mu Z^\nu). \tag{12}$$

Note that $\{\mathcal{O}_1, \mathcal{O}_2, \mathcal{O}_3, \mathcal{O}_4, \mathcal{O}_5\}$ and $\{\mathcal{O}_1, \mathcal{O}_2, \mathcal{O}_3, \mathcal{O}_5, \mathcal{O}_6\}$ are bases, but $\{\mathcal{O}_1, \mathcal{O}_2, \mathcal{O}_3, \mathcal{O}_4, \mathcal{O}_5, \mathcal{O}_6\}$ is a linearly dependent set.

Choosing $\{\mathcal{O}_1, \mathcal{O}_2, \mathcal{O}_3, \mathcal{O}_4, \mathcal{O}_5\}$ as our basis, we obtain the Lagrangian

$$\mathcal{L} \supset \sum_{i=1}^5 \kappa_i \mathcal{O}_i = -\kappa_1 \frac{M_Z^2}{v} X Z_\mu Z^\mu - \frac{\kappa_2}{2v} X F_{\mu\nu} F^{\mu\nu}$$

$$- \frac{\kappa_3}{2v} X F_{\mu\nu} \tilde{F}^{\mu\nu} \tag{13}$$

$$+ \frac{\kappa_4 M_Z^2}{M_X^2 v} \Box X Z_\mu Z^\mu + \frac{2\kappa_5}{v} X Z_\mu \Box Z^\mu. \tag{14}$$

The amplitude corresponding to this Lagrangian may be written as

$$\mathcal{A} = -\frac{2i}{v} \epsilon_1^{*\mu} \epsilon_2^{*\nu} (a_1 g_{\mu\nu} + a_2 p_{1\nu} p_{2\mu} + a_3 \epsilon_{\mu\nu\rho\sigma} p_1^\rho p_2^\sigma), \tag{15}$$

where

$$a_1 \equiv \kappa_1 M_Z^2 + (2(M_Z^2/M_X^2)\kappa_4 - \kappa_2) p_1 \cdot p_2$$
$$+ ((M_Z^2/M_X^2)\kappa_4 + \kappa_5)(p_1^2 + p_2^2), \tag{16}$$

$$a_2 \equiv \kappa_2, \tag{17}$$

$$a_3 \equiv \kappa_3. \tag{18}$$

TABLE I. A summary of the properties of the $\mathcal{O}_i$ operators considered in the text.

Operator	Dimension	CP	Gauge invariant
$\mathcal{O}_1$	3	Even	No
$\mathcal{O}_2$	5	Even	Yes
$\mathcal{O}_3$	5	Odd	Yes
$\mathcal{O}_4$	5	Even	No
$\mathcal{O}_5$	5	Even	No

Different operators (or equivalently, different amplitude structures) correspond to different symmetry properties, as is elucidated in Table I. Thus, for example, the most general *CP*-even coupling involves the four operators $\mathcal{O}_1$, $\mathcal{O}_2$, $\mathcal{O}_4$, and $\mathcal{O}_5$. The most general gauge-invariant coupling involves only $\mathcal{O}_2$ and $\mathcal{O}_3$. We emphasize also that this choice of operators allows one to parametrize all amplitude structures up to a given mass dimension. In particular, κ_1, κ_2, κ_4, and κ_5 can parametrize any Bose symmetric, Lorentz invariant kinematic function with mass dimension ≤ 2 for a_1, while retaining sufficient freedom to assign any possible constant value to a_2.[6]

III. GEOLOCATING: THE ON-PEAK CROSS SECTION

In Ref. [45], we provided a parameterization of XZZ couplings in terms of directions on a suitably defined sphere with a constant value for the on-peak ($M_{4\ell} = M_X$) cross section times branching ratio for the 4ℓ final state. We note in passing that this "geolocating" approach has the experimental benefit of making the normalization of the differential cross section used in the Matrix Element Method [128–136] trivial. To obtain the analogous "sphere" in the five-dimensional κ_i space corresponding to the Lagrangian in Eq. (14), we must determine the coefficients γ_{ij} in the equation

$$\Gamma(X \to ZZ \to 4\ell) = \Gamma_{SM} \sum_{i,j} \gamma_{ij} \kappa_i \kappa_j, \tag{19}$$

where $\Gamma(X \to ZZ \to 4\ell)$ is the partial width for $X \to ZZ^* \to 4\ell$ for the given final state ($4e$, 4μ or $2e2\mu$) after specified selections, Γ_{SM} is the value of this quantity for the tree-level SM ($\kappa_i = \delta_{i1}$), and the κ_i are defined by Eq. (14). We take $\gamma_{ij} = \gamma_{ji}$.

For any kinematic configuration with $M_{4\ell} = M_X$, the contributions to the amplitude from $\mathcal{O}_1$ and from $\mathcal{O}_4$ are equal. Thus

$$\gamma_{1j} = \gamma_{4j}, \tag{20}$$

---

[6]See Ref. [53] for a dictionary of conventions used for describing XZZ couplings in various works.

TABLE II. Numerical values for the coefficients defined in Eq. (19) that give the partial width for decay of the putative Higgs boson to the $2e2\mu$ final state with no event selection applied.

$\gamma_{11} = \gamma_{14} = \gamma_{44}$	γ_{22}	$\gamma_{12} = \gamma_{24}$	γ_{33}	$\gamma_{13} = \gamma_{23} = \gamma_{34} = \gamma_{35}$	γ_{25}	$\gamma_{15} = \gamma_{45}$	γ_{55}
1	0.090	−0.250	0.038	0	−0.250	0.978	0.987

and in particular $\gamma_{11} = \gamma_{14} = \gamma_{44} = 1$ (as $\gamma_{11} = 1$ by construction). Also, as the interference between parity-odd and parity-even amplitudes generically vanishes at the level of total cross sections, $\gamma_{3j} = 0$ for $j \neq 3$. Thus, the only γ_{ij} which we need to calculate, beyond those provided in Ref. [45], are γ_{15}, γ_{25}, and γ_{55}. For convenience, we present all γ_{ij} for the $2e2\mu$ final state without event selection in Table II. In general these values depend both on the choice of four-lepton final state and the event selection applied.

It is interesting that γ_{55} is close to, but slightly less than, 1. We therefore explore how this value arises. In general,

$$\frac{\Gamma_B}{\Gamma_A} = \frac{1}{\Gamma_A} \int \frac{d\Gamma_B}{d\mathbf{x}} d\mathbf{x} = \int \left(\frac{d\Gamma_B}{d\mathbf{x}} \Big/ \frac{d\Gamma_A}{d\mathbf{x}} \right) \left(\frac{d\Gamma_A}{d\mathbf{x}} \Big/ \Gamma_A \right) d\mathbf{x}$$
$$= \left\langle \left(\frac{d\Gamma_B}{d\mathbf{x}} \Big/ \frac{d\Gamma_A}{d\mathbf{x}} \right) \right\rangle_A; \qquad (21)$$

that is, the ratio of widths is given by the expectation value of the ratio of differential widths as found using the appropriate hypothesis. If $d\Gamma_i/d\mathbf{x}$ is the differential width for some set of kinematic variables, $\mathbf{x}$, when $\kappa_i = 1$ and $\kappa_j = 0$ for $j \neq i$, then we find

$$\left(\frac{d\Gamma_5}{d\mathbf{x}} \Big/ \frac{d\Gamma_1}{d\mathbf{x}} \right) = \left(\frac{M_{Z_1}^2 + M_{Z_2}^2}{M_Z^2} \right)^2, \qquad (22)$$

where $M_{Z_{1(2)}}$ is the invariant mass of the heavier (lighter) lepton pair. Thus
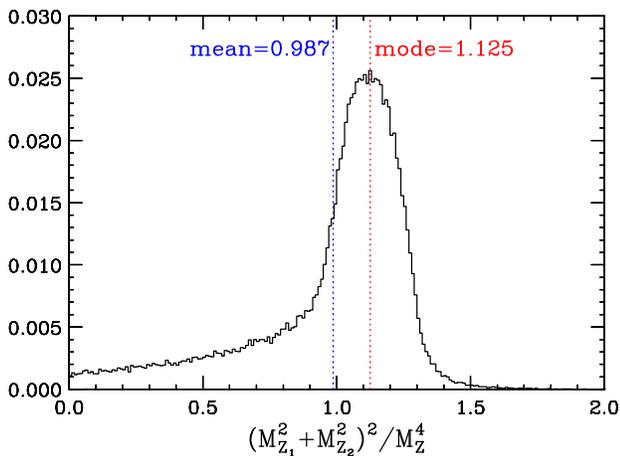
FIG. 1 (color online). The distribution of the quantity $(M_{Z_1}^2 + M_{Z_2}^2)^2/M_Z^4$, which is the ratio of differential cross sections due to the operator $\mathcal{O}_5$ and due to the SM operator, $\mathcal{O}_1$, as evaluated for SM events [see Eqs. (22) and (23)]. The mean of this quantity is equal to γ_{55}.

$$\gamma_{55} = \left\langle \left(\frac{M_{Z_1}^2 + M_{Z_2}^2}{M_Z^2} \right)^2 \right\rangle_{\rm SM}. \qquad (23)$$

As for most events with $M_{4\ell} \approx M_X$, $M_{Z_1} \approx M_Z$ and $M_{Z_2} \lesssim M_X - M_Z$, so with $M_X = 125$ one would expect $(M_{Z_1}^2 + M_{Z_2}^2)^2/M_Z^4 \approx 1.1$–1.3, which disagrees with our result for γ_{55} in Table II. However, this is a naive expectation. Figure 1 illustrates that while the peak of the distribution of $(M_{Z_1}^2 + M_{Z_2}^2)^2/M_Z^4$ for SM events is 1.125, a long tail extends to very low values of this quantity. This tail lowers the average value of the quantity, and hence of γ_{55} to 0.987, as shown in Table II. We note that in this paper we utilize the event generators MadGraph5 [137] and CalcHEP [138] using a model file created with FeynRules [139].

We have presented the γ_{ij} corresponding to a particular Higgs boson width in the limit of no event selection; a more realistic analysis should include the event selection, efficiencies, etc. We emphasize that the three operators ($\mathcal{O}_1$, $\mathcal{O}_2$, and $\mathcal{O}_3$) that were the focus in Ref. [45], and which have been the focus of most experimental and theoretical analyses thus far, do not exhaust all the possibilities. Even if studies of these three operators seem to indicate a SM-like Higgs boson, one must still probe the complementary $(\kappa_1, \kappa_4, \kappa_5)$ space to conclusively establish the boson's identity.

IV. OFF-SHELL PHENOMENOLOGY OF *XZZ* OPERATORS

A. Invariant mass dependence of off-shell cross sections

As noted above, there has been much interest recently in using four-lepton events from off-shell Higgs boson production, i.e. events with $M_{4\ell} \gg M_X$, to constrain the total Higgs boson width [30,49,56,67–69]. We point out here that, for a fixed value of the $X \to ZZ$ partial width (19) (or sphere of fixed radius in geolocating language), the off-shell $X^* \to ZZ$ cross section due to any of the dimension-five operators (7)–(12) is much higher than in the Standard Model. The experimental sensitivity to this off-shell production is greatly enhanced through interference with the NLO $gg \to ZZ$ background [30,49,56,67–69,140–148], so determining the precise experimental sensitivity to some nonstandard *XZZ* couplings is somewhat nontrivial. In this paper, we consider only the enhancement in cross sections relative to the Standard Model that is attained with these operators; a detailed study of the sensitivity, including the effects of interference, will be treated in future work.

Before proceeding, we consider the obvious question of what value of the ggX coupling to use. In the Standard Model, the ggX coupling is given by

$$g_{ggX}(M_{4\ell}) = \frac{\alpha_s(M_{4\ell})}{4\pi v} \sum_Q A^H_{1/2}(\tau_Q) \qquad (24)$$

at one loop, where

$$A^H_{1/2}(\tau) = 2[\tau + (\tau - 1)f(\tau)]\tau^{-2}, \qquad (25)$$

$f(\tau)$ is defined by

$$f(\tau) = \begin{cases} \arcsin^2\sqrt{\tau} & \tau \le 1 \\ -\frac{1}{4}\left[\log\frac{1+\sqrt{1-\tau^{-1}}}{1-\sqrt{1-\tau^{-1}}} - i\pi\right]^2 & \tau > 1 \end{cases}, \qquad (26)$$

and $\tau_Q = M^2_{4\ell}/4M^2_Q$, following the expressions in e.g. Refs. [149,150]. This expression, more frequently viewed as describing the evolution of the ggH coupling with M_H, can be interpreted somewhat more generally, as it gives the value of this coupling at a particular value of invariant mass, regardless of the on-shell mass of the resonance.

However, if we are introducing (in some cases radically) new physics in the XZZ couplings, we cannot necessarily assume that the SM expression for the ggX coupling will hold. Therefore, we consider an alternative hypothesis that the ggX coupling is fixed at all scales to its SM value at 125 GeV. We show the LO cross sections σ_{1-5} as a function of $M_{4\ell}$ for the five "pure" operators $\mathcal{O}_{1-5}$ in Fig. 2, in which
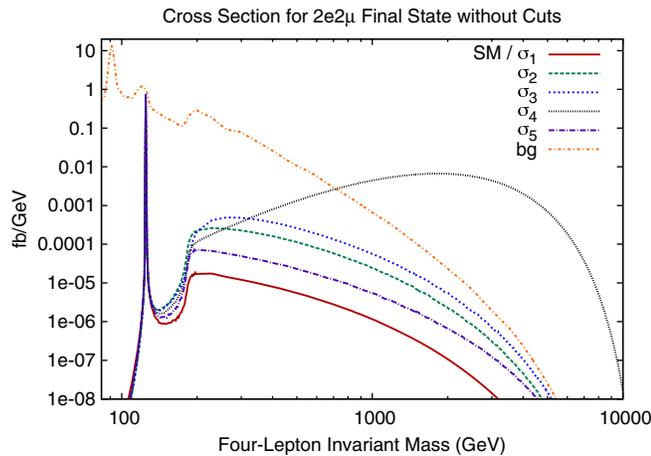
FIG. 2 (color online). The differential cross section as a function of four-lepton invariant mass for $2e2\mu$ events before event selections. Results are shown for pure $\mathcal{O}_1$, $\mathcal{O}_2$, $\mathcal{O}_3$, $\mathcal{O}_4$, and $\mathcal{O}_5$ couplings [cf. Eq. (14)], as well as for the irreducible $q\bar{q} \to ZZ \to 2e2\mu$ background (bg). There is no event selection applied to the signal events; for the background, a minimal $M_{l\bar{l}} > 1$ GeV selection is applied to avoid infrared divergences. For each signal hypothesis, the normalization has been chosen to be equal to the entire SM on-peak Higgs boson cross section in this channel. In this figure, the ggX coupling is taken to be constant with respect to invariant mass.

the ggX coupling does not evolve with $M_{4\ell}$. In Fig. 3, we show these same cross sections, but now calculated with a coupling that evolves according to Eq. (24). Explicitly, σ_i is the cross section, in a particular ggX coupling scenario, when $\kappa_i = \gamma_{ii}^{-1/2}$ and $\kappa_j = 0$ for $i \ne j$. This choice of κ_i serves to normalize the cross sections, so that the SM value for cross section times branching ratio for $M_{4\ell} \approx 125$ GeV is obtained. Signal and background rates integrated over a range of off-shell invariant masses are provided in Table III. We note from this table, and from Figs. 2 and 3 above, that σ_{2-5} are significantly larger than σ_1, the SM off-shell cross section, though the overall scale of cross sections is relatively small, with the exception of σ_4. While, as noted above, we cannot translate these observations directly into a sensitivity, largely because of the importance of interference with the $gg \to ZZ$ continuum background, it is clear that the off-shell cross sections provide a source of information about the tensor XZZ couplings that is complementary to data obtained on the Higgs boson mass peak. As the large values of σ_4 are symptomatic of potential unitarity-violating behavior, in Subsec. IV C we will quantify the reduction of the cross section for $\mathcal{O}_4$ when one only integrates over values of invariant mass consistent with unitarity requirements.

B. Analytic expressions for off-peak cross sections

To gain a greater understanding of the behavior of the various cross sections at large invariant mass, we obtain analytic expressions for the partonic differential cross section $\frac{d\hat{\sigma}(\hat{s})}{dM_{Z_1}dM_{Z_2}}$. These expressions are valid in general, though we have suppressed the dependence on the Higgs boson width, as our interest is in the regime where the Higgs boson is not on shell. Specifically, we find that
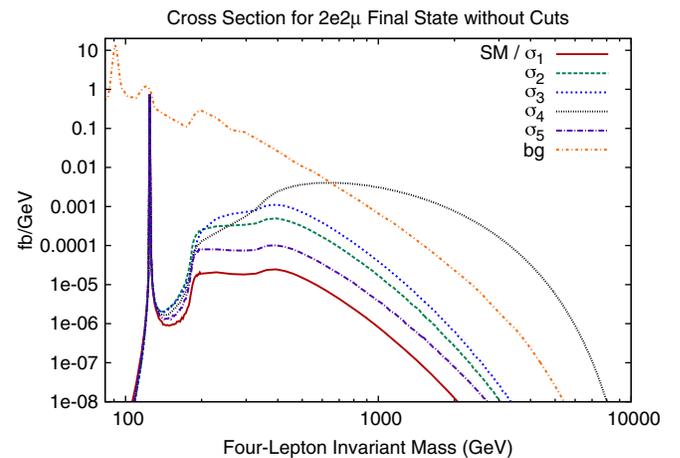
FIG. 3 (color online). The same as Fig. 2, but in this figure, the ggX coupling evolves with invariant mass according to the expression in Eq. (24).

TABLE III.   Integrated cross sections in femtobarns for the $2e2\mu$ final state without event selections for various signal processes and the LO irreducible background. The signal cross sections have been normalized to give the SM Higgs boson on-resonance cross section. Values are given both for a fixed ggX coupling and assuming the SM evolution of this quantity with invariant mass.

Operator	$\sigma > M_X$, fixed g_{ggX}	$\sigma > 250$ GeV, fixed g_{ggX}	$\sigma > M_X$, $g_{ggX}(M_{4\ell})$	$\sigma > 250$ GeV, $g_{ggX}(M_{4\ell})$
$\mathcal{O}_1$	0.005	0.004	0.009	0.008
$\mathcal{O}_2$	0.099	0.083	0.171	0.152
$\mathcal{O}_3$	0.206	0.186	0.366	0.341
$\mathcal{O}_4$	18.2	18.2	4.54	4.53
$\mathcal{O}_5$	0.023	0.018	0.037	0.032
LO BG	38.8	13.1	38.8	13.1

$$\frac{d\hat{\sigma}(\hat{s})}{dM_{Z_1}dM_{Z_2}} = g_{ggX}^2 (g_L^2 + g_R^2)^2 \left(\frac{M_{Z_1}^5 M_{Z_2}^5 \sqrt{x}}{2^{14} 3^2 \pi^5 v^2 \hat{s}^2} \right) \left(\frac{\hat{s}}{\hat{s} - M_X^2} \right)^2 \left(\frac{(2M_{Z_1} dM_{Z_1})(2M_{Z_2} dM_{Z_2})}{(M_{Z_1}^2 - M_Z^2)^2 + M_Z^2 \Gamma_Z^2)(M_{Z_2}^2 - M_Z^2)^2 + M_Z^2 \Gamma_Z^2)} \right) \sum_{i,j} \kappa_i \kappa_j \chi_{ij}, \quad (27)$$

where, using the coupling of the Z to charged leptons, we have that

$$g_L^2 + g_R^2 = 16\pi^2 \alpha_{EM}(\hat{s})^2 \left(\frac{2\sin^4\theta_W - \sin^2\theta_W + 1/4}{\sin^2\theta_W \cos^2\theta_W} \right), \quad (28)$$

and x is defined, analogously to Refs. [19,34], by

$$x = \left(\frac{\hat{s} - M_{Z_1}^2 - M_{Z_2}^2}{2M_{Z_1} M_{Z_2}} \right)^2 - 1. \quad (29)$$

The expressions for the unique, nonvanishing χ_{ij} are

$$\chi_{11} = (3+x) \left(\frac{M_Z^2}{M_{Z_1} M_{Z_2}} \right)^2, \quad (30)$$

$$\chi_{12} = -\frac{3}{2} \left(\frac{M_Z^2}{M_{Z_1} M_{Z_2}} \right)^2 \left(\frac{\hat{s}}{M_Z^2} - \frac{M_{Z_1}^2 + M_{Z_2}^2}{M_Z^2} \right), \quad (31)$$

$$\chi_{14} = (3+x) \left(\frac{M_Z^2}{M_{Z_1} M_{Z_2}} \right)^2 \left(\frac{\hat{s}}{M_X^2} \right), \quad (32)$$

$$\chi_{15} = (3+x) \left(\frac{M_Z^2}{M_{Z_1} M_{Z_2}} \right)^2 \left(\frac{M_{Z_1}^2 + M_{Z_2}^2}{M_Z^2} \right), \quad (33)$$

$$\chi_{22} = 3 + 2x, \quad (34)$$

$$\chi_{24} = -\frac{3}{2} \left(\frac{M_Z^2}{M_{Z_1} M_{Z_2}} \right)^2 \left(\frac{\hat{s}}{M_X^2} \right) \left(\frac{\hat{s}}{M_Z^2} - \frac{M_{Z_1}^2 + M_{Z_2}^2}{M_Z^2} \right), \quad (35)$$

$$\chi_{25} = -\frac{3}{2} \left(\frac{M_Z^2}{M_{Z_1} M_{Z_2}} \right)^2 \left(\frac{M_{Z_1}^2 + M_{Z_2}^2}{M_Z^2} \right) \left(\frac{\hat{s}}{M_Z^2} - \frac{M_{Z_1}^2 + M_{Z_2}^2}{M_Z^2} \right), \quad (36)$$

$$\chi_{33} = 2x, \quad (37)$$

$$\chi_{44} = (3+x) \left(\frac{M_Z^2}{M_{Z_1} M_{Z_2}} \right)^2 \left(\frac{\hat{s}}{M_X^2} \right)^2, \quad (38)$$

$$\chi_{45} = (3+x) \left(\frac{M_Z^2}{M_{Z_1} M_{Z_2}} \right)^2 \left(\frac{M_{Z_1}^2 + M_{Z_2}^2}{M_Z^2} \right) \left(\frac{\hat{s}}{M_X^2} \right), \quad (39)$$

$$\chi_{55} = (3+x) \left(\frac{M_Z^2}{M_{Z_1} M_{Z_2}} \right)^2 \left(\frac{M_{Z_1}^2 + M_{Z_2}^2}{M_Z^2} \right)^2. \quad (40)$$

We have defined these quantities such that $\chi_{ij} = \chi_{ji}$. Note that $\chi_{i3} = 0$ for $i \neq 3$, essentially due to the parity properties of the operators. Equation (27) is normalized for the $4e$ or 4μ final state (though it does not include the effects of interference between lepton pairs; see, e.g. Ref. [40] for more discussion of this effect). To obtain the differential cross section for the $2e2\mu$ final state, one must multiply by 2.

We now proceed to obtain expressions for the partonic cross section, $\hat{\sigma}(\hat{s})$, by using the narrow width approximation to integrate over M_{Z_1} and M_{Z_2}. The result is that

$$\hat{\sigma}(\hat{s}) = g_{ggX}^2 \left(\frac{\sqrt{1 - 4M_Z^2/\hat{s}} M_Z^4}{512\pi v^2 \hat{s}} \right) \left(\frac{\hat{s}}{\hat{s} - M_X^2} \right)^2 \times \sum_{i,j} \kappa_i \kappa_j \xi_{ij} (\mathrm{BR}(Z \to l^+ l^-))^2, \quad (41)$$

where $\mathrm{BR}(Z \to l^+ l^-)$ gives the branching ratio for Z decay to a specific lepton flavor. As in Eq. (30), this expression gives the cross section for the $4e$ or 4μ final states; the value for the $2e2\mu$ final state is greater by a factor of 2. The ξ_{ij} can be found using the expression

$$\xi_{ij} = \lim_{M_{Z_{1,2}} \to M_Z} \chi_{ij}. \tag{42}$$

Explicitly, the values of ξ_{ij} are

$$\xi_{11} = \frac{\hat{s}^2}{4M_Z^4} - \frac{\hat{s}}{M_Z^2} + 3, \tag{43}$$

$$\xi_{12} = -\frac{3\hat{s}}{2M_Z^2} + 3, \tag{44}$$

$$\xi_{14} = \left(\frac{\hat{s}}{M_X^2}\right)\left(\frac{\hat{s}^2}{4M_Z^4} - \frac{\hat{s}}{M_Z^2} + 3\right), \tag{45}$$

$$\xi_{15} = 2\left(\frac{\hat{s}^2}{4M_Z^4} - \frac{\hat{s}}{M_Z^2} + 3\right), \tag{46}$$

$$\xi_{22} = \frac{\hat{s}^2}{2M_Z^4} - \frac{2\hat{s}}{M_Z^2} + 3, \tag{47}$$

$$\xi_{24} = \left(\frac{\hat{s}}{M_X^2}\right)\left(-\frac{3\hat{s}}{2M_Z^2} + 3\right), \tag{48}$$

$$\xi_{25} = 2\left(-\frac{3\hat{s}}{2M_Z^2} + 3\right) \tag{49}$$

$$\xi_{33} = \frac{\hat{s}^2}{2M_Z^4} - \frac{2\hat{s}}{M_Z^2}, \tag{50}$$

$$\xi_{44} = \left(\frac{\hat{s}}{M_X^2}\right)^2\left(\frac{\hat{s}^2}{4M_Z^4} - \frac{\hat{s}}{M_Z^2} + 3\right), \tag{51}$$

$$\xi_{45} = 2\left(\frac{\hat{s}}{M_X^2}\right)\left(\frac{\hat{s}^2}{4M_Z^4} - \frac{\hat{s}}{M_Z^2} + 3\right), \tag{52}$$

$$\xi_{55} = 4\left(\frac{\hat{s}^2}{4M_Z^4} - \frac{\hat{s}}{M_Z^2} + 3\right). \tag{53}$$

We note that many of these expressions can be obtained from the relations

$$\xi_{i4} = (\hat{s}/M_X^2)\xi_{i1} \tag{54}$$

and

$$\xi_{i5} = 2\xi_{i1}. \tag{55}$$

As was the case for χ_{ij}, $\xi_{ij} = \xi_{ji}$ and $\xi_{i3} = 0$ when $i \neq 3$.

Some observations about the cross sections from the various operators are as follows:

(1) $\mathcal{O}_2$: As noted above, the value of κ_2 which gives the SM partial width when all other couplings vanish is $\kappa_2 = \gamma_{22}^{-1/2}$. (See Table II for the values of the γ_{ij}.) Thus, in the high invariant mass limit,

$$\lim_{\sqrt{\hat{s}} \to \infty} \frac{\sigma_2(\sqrt{\hat{s}})}{\sigma_1(\sqrt{\hat{s}})} = \frac{1}{\gamma_{22}} \lim_{\sqrt{\hat{s}} \to \infty} \frac{\xi_{22}(\sqrt{\hat{s}})}{\xi_{11}(\sqrt{\hat{s}})} = \frac{2}{\gamma_{22}} \approx 22. \tag{56}$$

Naively, it might be surprising that ξ_{22}/ξ_{11} asymptotes to a constant value in the high $\sqrt{\hat{s}} = M_{4\ell}$ limit, as $\mathcal{O}_2$ is built of the operators given in (2) and (3) that are higher dimensional than $\mathcal{O}_1$. However, the contributions to the helicity amplitudes from these higher-dimensional operators which depend on the highest powers of $\hat{s}$ cancel. This cancellation is related to the preservation of unitarity by gauge invariant operators.

(2) $\mathcal{O}_3$: Using the analogous procedure, we find that

$$\lim_{\sqrt{\hat{s}} \to \infty} \frac{\sigma_3(\sqrt{\hat{s}})}{\sigma_1(\sqrt{\hat{s}})} = \frac{2}{\gamma_{33}} \approx 53. \tag{57}$$

Again, the fact that the highest power of $\hat{s}$ in ξ_{33} is 2 is related to the gauge invariance of the $\mathcal{O}_3$ operator.

(3) $\mathcal{O}_4$: Here there is a dramatic enhancement of the cross section at high energies as

$$\lim_{\sqrt{\hat{s}} \to \infty} \frac{\sigma_4(\sqrt{\hat{s}})}{\sigma_1(\sqrt{\hat{s}})} = \frac{\hat{s}^2}{M_X^4}. \tag{58}$$

The tendency for amplitudes associated with this operator to grow with energy leads to issues with unitarity, as we will discuss in more detail in Subsec. IV C.

(4) $\mathcal{O}_5$: If we use the expressions for ξ_{11} and ξ_{55} in Eqs. (43) and (53), then we would obtain

$$\lim_{\sqrt{\hat{s}} \to \infty} \frac{\sigma_5(\sqrt{\hat{s}})}{\sigma_1(\sqrt{\hat{s}})} = \frac{4}{\gamma_{55}} \approx 4. \tag{59}$$

However, following Eqs. (31) and (40), we note that

$$\frac{\chi_{55}}{\chi_{11}} = \left(\frac{M_{Z_1}^2 + M_{Z_2}^2}{M_Z^2}\right)^2. \tag{60}$$

The extra powers of M_{Z_1} and M_{Z_2} in χ_{55} mean that the narrow width approximation (NWA), which was used in obtaining the ξ_{ij} from the χ_{ij}, breaks down, leading to an enhancement of the cross section at high invariant mass from events with very off-shell Z bosons. The prevalence of events with very off-shell (high invariant mass) Z bosons can be seen in Fig. 4; the enhancement of the partonic cross section as a function of $\hat{s}$ is shown in Fig. 5. The enhancement in cross section versus the NWA expectation for $\mathcal{O}_5$ might seem to promise an increase in sensitivity. However, the interference between signal events with large, off-shell M_{Z_1} and M_{Z_2} and the continuum $gg \to ZZ$ will be quite small, and the total cross section for such events is small for LHC purposes. Perhaps the situation will be somewhat more optimistic at a 100 TeV collider.
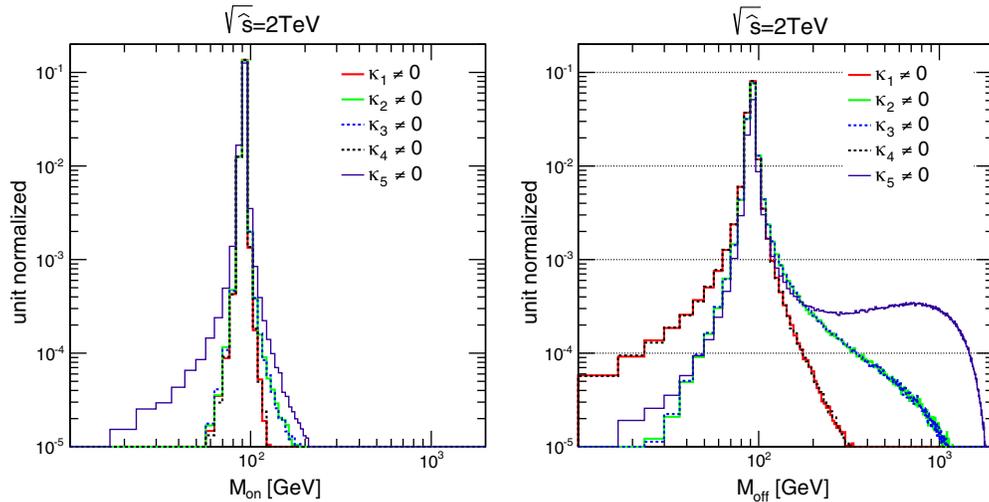
FIG. 4 (color online). The distribution of Z invariant mass for the Z with invariant mass closest to M_Z ($M_{\rm ON}$, left) and the Z with invariant mass furthest from M_Z ($M_{\rm OFF}$, right), in $gg \to X \to ZZ \to 2e2\mu$ events with $\hat{s} = 2$ TeV. The curve labeled "$\kappa_i \neq 0$" is the distribution for which κ_i is nonvanishing but $\kappa_j = 0$ for $i \neq j$; these curves have the same colors as the corresponding curves in Figs. 2 and 3. We learn that a significant fraction of events from $\mathcal{O}_5$, and to a lesser extent $\mathcal{O}_2$, involve very off-shell Z bosons.

C. Unitarity bounds on $\mathcal{O}_4$

A striking feature in Figs. 2 and 3, as well as in the integrated cross sections in Table III, is the rapidly growing cross section from the $\mathcal{O}_4$ operator. However, the growth in the strength of this operator with invariant mass will lead to amplitudes which violate partial wave unitarity at some mass scale Λ [117,151–153]. Three approaches to this issue are, in increasing order of conservatism,

(1) Ignore unitarity and set limits using the entire predicted off-shell cross section.
(2) Use form factors, e.g. as in Ref. [154,155], that prevent the amplitude from violating unitarity, or at least increase the mass scale at which unitarity is violated.

(3) Consider only cross sections for invariant masses less than Λ.

We demonstrate how one obtains the predicted off-shell cross section in each of these approaches in Fig. 6. We note that options 2 and 3 both require a study of the unitarity bounds on κ_4.

Unitarity-violating behavior can be probed in a variety of channels [117,149,151–153]. As we have specified only an effective theory of the XZZ coupling, we will look only at $Z_L Z_L \to Z_L Z_L$ scattering, as our study of this process
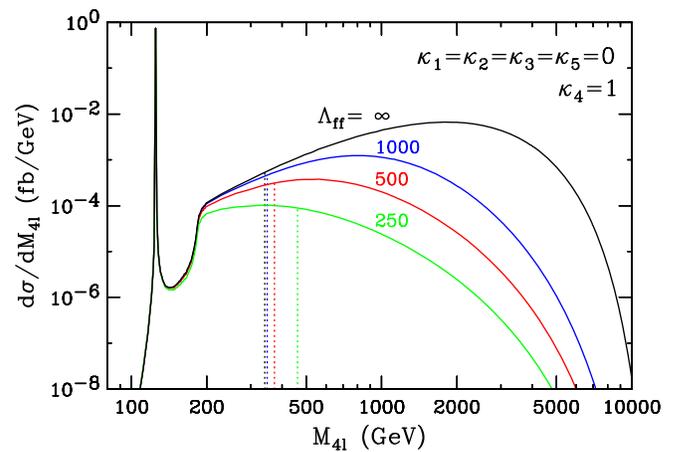
FIG. 6 (color online). The differential cross section $d\sigma/dM_{4\ell}$ in fb/GeV for a pure $\mathcal{O}_4$ operator with $\kappa_4 = 1$, for several choices of the form-factor scale Λ_{ff}: ∞ (black line), 1 TeV (blue line), 500 GeV (red line), and 250 GeV (green line). The vertical dotted lines denote the scale Λ at which unitarity violation occurs in each case. The cross section considered (and listed in Table IV) in each form-factor scenario is that found by integrating under the relevant cross section curve up to the relevant dotted line.

FIG. 5 (color online). The ratio between the actual partonic $gg \to ZZ^* \to 2e2\mu$ cross section for pure $\mathcal{O}_5$ couplings, and the value of this partonic cross section calculated in Eq. (43) using the narrow width approximation (NWA).

requires no assumptions beyond the Lagrangian presented above in Eq. (14). However, in the well-motivated limit where $SU(2)$ symmetry is spontaneously broken, we would expect the XWW couplings to be related, allowing the study of additional channels.

Longitudinal ZZ scattering involves three diagrams; s-, t-, and u-channel scalar exchange. In the limit where M_Z (and, of course, Γ_H) can be neglected, the contribution to the $J = 0$ partial wave when κ_4 is nonzero, $\kappa_2 = \kappa_3 = \kappa_5 = 0$, and $\kappa_1 = 1 - \kappa_4$ (to ensure that one obtains the SM value of the partial width), is

$$a_0(s) = \left(\frac{M_X^2}{32\pi v^2}\right)\left[\frac{(s/M_X^2)^2}{6}((10 - 3s/M_X^2)\kappa_4^2 - 20\kappa_4)\right.$$

(61)

$$\left. - \left(3 + \frac{M_X^2}{s - M_X^2} - \frac{2M_X^2}{s}\log\left(1 + \frac{s}{M_X^2}\right)\right)\right], \quad (62)$$

where we have included the factor of $1/2$ from the normalization of ZZ in our expression for a_0 [149,151].

Even for relatively moderate values of $\sqrt{s}$, $a_0(s)$ is dominated by the κ_4^2 and κ_4 terms. Clearly, at very high values of s, we have

$$a_0(s) \sim \frac{-s^3\kappa_4^2}{64\pi M_X^4 v^2}.$$

(63)

Thus, the s dependence of this quantity is three powers greater than for its SM analogue, which asymptotes to a constant value. Two of these three additional powers are due to the s dependence of the $\mathcal{O}_4$ vertex, while the third is due to a failure of the unitarity-preserving cancellation between amplitudes that cause the SM amplitude to approach a constant at high energies.

Using expression (63), an approximate unitarity bound found by setting $|\text{Re}\,a_0(\Lambda^2)| = 1/2$ (cf. Ref. [149]) is

$$\Lambda = (32\pi M_X^4 v^2)^{1/6}|\kappa_4|^{-1/3}.$$

(64)

As $(32\pi M_X^4 v^2)^{1/6} \approx 340$ GeV, it is clear that we cannot neglect the other terms in $a_0(s)$.

Considering now the entire term proportional to κ_4^2 in Eq. (61), we note that for either sign of κ_4, this term is positive for $s < \sqrt{10/3}M_H \approx 230$ GeV and negative thereafter. The term linear in κ_4 gives a negative contribution when κ_4 is positive and a positive contribution when κ_4 is negative. Thus, if $\kappa_4 > 0$ (and if the unitarity bound Λ is greater than ≈ 230 GeV), then the unitarity bound will occur when $a_0(s)$ becomes sufficiently *negative*, i.e. when
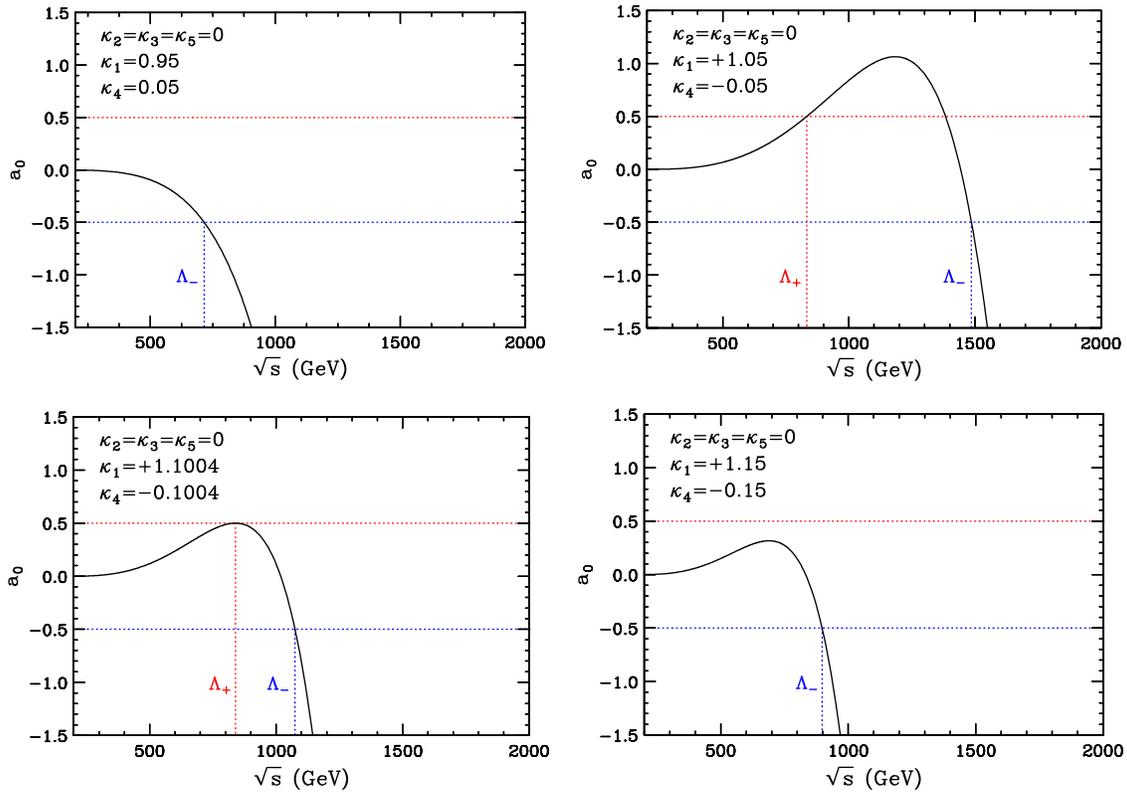
FIG. 7 (color online). The contribution to the $J = 0$ partial wave for the $Z_L Z_L \rightarrow Z_L Z_L$ scattering amplitude, $a_0(s)$, shown as a function of $\sqrt{s}$ for several different values of κ_4 to illustrate the qualitative differences in the behavior of this function for different values of κ_4. In all cases $\kappa_1 = 1 - \kappa_4$ to ensure that the point considered gives the SM partial width.
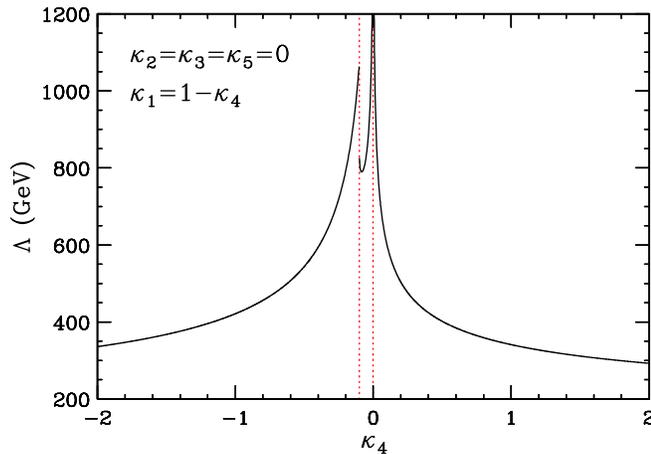
FIG. 8 (color online).   The unitarity violation scale Λ (in GeV) as a function of κ_4, for an admixture of κ_1 and κ_4 couplings. As above, $\kappa_1 = 1 - \kappa_4$ so that one obtains the SM value for the $X \to 4\ell$ partial width.

TABLE IV.   Integrated cross sections in femtobarns (at leading order) for the $2e2\mu$ final state without event selections and for the case of a pure $\mathcal{O}_4$ operator, with different values of the form-factor scale Λ_{ff}. The signal cross sections have been normalized to give the SM Higgs boson on-resonance cross section. The first values are obtained with a fixed ggX coupling, while the values in parentheses assume the SM evolution of this quantity with invariant mass. The second column shows the scale Λ of unitarity violation. The results in the third (fourth) column are obtained after integrating over the whole allowed range for $M_{4\ell}$ (only up to $M_{4\ell} \leq \Lambda$).

Λ_{ff} (GeV)	Λ (GeV)	$\sigma > M_X$, all $M_{4\ell}$ (fb)	$\sigma > M_X$, for $M_{4\ell} \leq \Lambda$ (fb)
∞	341.3	18.205 (4.544)	0.044 (0.065)
1000	349.2	1.526 (1.435)	0.043 (0.065)
500	373.0	0.333 (0.472)	0.038 (0.065)
250	461.8	0.064 (0.107)	0.026 (0.053)

$a_0(\Lambda^2) = -1/2$. However, if $\kappa_4 < 0$, then $a_0(s)$ will be positive up to some scale > 230 GeV, and possibly much greater. At sufficiently high values of s, the curve must turn negative and approach expression (63) at high energies. So the minimal (and hence the physically interesting) scale at which partial wave unitarity is violated may occur for either positive or negative values of $a_0(s)$. Defining $\Lambda_{\pm}$ to be the lowest value of $\sqrt{s}$ for which $a_0(s) = \pm 1/2$, we demonstrate the behavior of $a_0(s)$ for various choices of κ_4 in Fig. 7. We find numerically that when Λ_+ exists, it is often approximately equal to Λ_{linear}, the value of the unitarity bound if $a_0(s)$ contained only the term linear in κ_4, while Λ_- is generally closer to Λ_{quad}, the value of the unitarity bound if $a_0(s)$ contained only the term quadratic in κ_4.

Based on this understanding of the behavior of $a_0(s)$ for various values of κ_4, a unitarity bound as a function of κ_4 can be determined, which is shown in Fig. 8. We note that the transition from the region where the unitarity bound is $\approx \Lambda_{\text{quad}}$ to the region where the unitarity bound is $\approx \Lambda_{\text{linear}}$ at $\kappa_4 = \kappa_{4,\text{special}}$ provides a "first-order transition." This is because for values of κ_4 slightly greater than the values at this point, $|a_0(s)| = 1/2$ for both positive and negative values of $a_0(s)$, while for values slightly less than the values at this point, $|a_0(s)| = 1/2$ only occurs when $a_0(s) = -1/2$. At this point, $\kappa_{4,\text{special}} \approx -0.1004$, the maximum of $a_0(s)$ is equal to $1/2$, as may be seen in the bottom-left plot in Fig. 7.

In a conservative approach to taming the high-energy behavior of $\mathcal{O}_4$, we only consider events with $M_{4\ell} < \Lambda(\kappa_4)$ when excluding a particular value of κ_4. A less conservative approach is to consider a "form-factor" scenario in κ_4 depends on s as follows:

$$\kappa_4 \to \frac{1 + M_X^2/\Lambda_{ff}^2}{1 + s/\Lambda_{ff}^2} \times \kappa_4. \qquad (65)$$

The expression in the numerator is only a normalization used to ensure that $\kappa_4(M_X)$ is unchanged by the transformation. As noted above, the high-energy behavior of $a_0(s)$, in the absence of form factors, goes as the third power of s. Hence, the transformation in Eq. (65) does not fully unitarize $Z_L Z_L$ scattering. Therefore, in employing this procedure, we consider only the cross section integrated up to the unitarity bound found when the coupling is modified as in Eq. (65). We also modify the $gg \to X \to ZZ^* \to 4\ell$ cross section accordingly, as can be seen in Fig. 6.

Cross sections obtained from this procedure are shown in Table IV and Fig. 9 for several choices of the form-factor scale Λ_{ff}. We have also included the cross section found from the unitarity bounds in the case where we do not modify κ_4; this corresponds to the $\Lambda_{ff} \to \infty$ limit. We note that these cross sections are quite modest, especially compared with the value for σ_4 shown in Table III above ($18.2/4.54$ fb in the fixed/evolving ggX coupling scenario).

However, the off-shell cross section for a pure $\mathcal{O}_4$ coupling is still significantly larger than the SM off-shell cross section ($5/9$ ab in the fixed/evolving ggX coupling scenario, as given in Table III). As it was suggested in Ref. [56] that the LHC may be sensitive ultimately to an off-shell cross section 5 to 10 times greater than the SM value, there is reason to hope that one can discriminate between $\mathcal{O}_1$ and $\mathcal{O}_4$, even when taking unitarity into account in a conservative manner.

V. ON-SHELL PHENOMENOLOGY OF XZZ OPERATORS

Now that we have shown the importance of the off-shell ($M_{4\ell} \gg M_X$) four-lepton cross section for probing XZZ couplings, we proceed to make a few remarks about the relevant on-shell phenomenology, focusing, in particular, on probing $\mathcal{O}_5$ couplings. We note that interference with
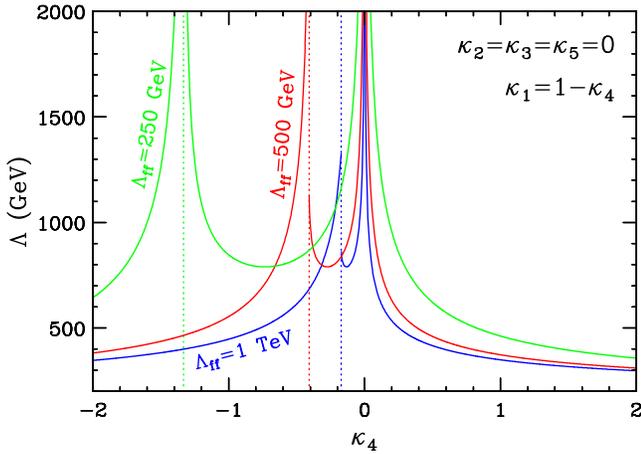
FIG. 9 (color online).   The same as Fig. 8, but in the presence of a form factor with $\Lambda_{ff} = 1$ TeV (blue), $\Lambda_{ff} = 500$ GeV (red), and $\Lambda_{ff} = 250$ GeV (green).

continuum $gg \to ZZ$ is less important here than in the off-shell case considered above due to one of the Z bosons necessarily being off shell.

A. Distinguishing $\mathcal{O}_5$ on peak

Let $\mathcal{A}_{1(5)}$ refer to the amplitude for a particular kinematic configuration due to $\mathcal{O}_{1(5)}$. Then

$$\mathcal{A}_5 = \frac{M_{Z_1}^2 + M_{Z_2}^2}{M_Z^2} \mathcal{A}_1, \qquad (66)$$

as alluded to above. Thus, when $M_{4\ell} \approx M_X$, the dependence of the amplitude on $M_{Z_1}^2 + M_{Z_2}^2$ will affect the angular and invariant distributions of the four leptons, in particular
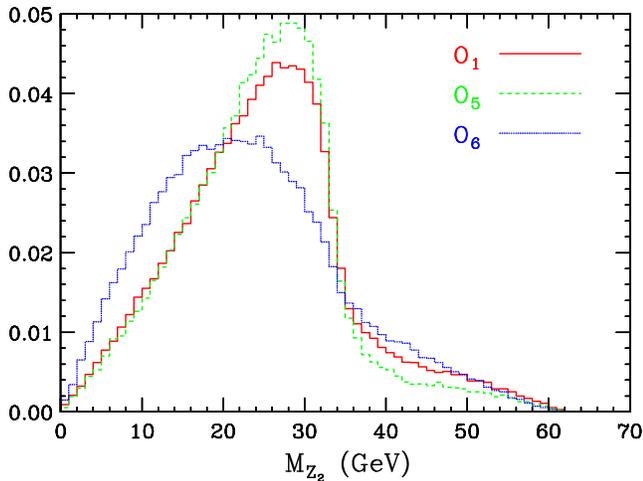
FIG. 10 (color online).   This figure shows the invariant mass distribution for the reconstructed Z with lower invariant mass (M_{Z_2}) for pure $\mathcal{O}_1$ (tree-level SM) couplings (red solid line), pure $\mathcal{O}_5$ couplings (green dashed line), and pure $\mathcal{O}_6$ couplings (blue dotted line).

the M_{Z_2} distribution. To demonstrate this, we compare the M_{Z_2} distribution due to pure $\mathcal{O}_1$, $\mathcal{O}_5$, and $\mathcal{O}_6$ couplings in Fig. 10. We note that while there is a discernible difference between the SM $\mathcal{O}_1$ distribution and the $\mathcal{O}_5$ distribution, this difference is relatively subtle, which suggests that it may be somewhat challenging to discover or constrain κ_5 couplings at the LHC. We give some idea of the extent to which this is true in the next subsection.

B. Quantifying sensitivity to non-SM couplings

The optimal discrimination between two hypotheses is that obtained using the likelihood as the test statistic [156]. With this in mind, we can quantify the maximum possible sensitivity for the exclusion of non-SM Higgs boson couplings to Z bosons by determining the average value of the log likelihood ratio using SM events, namely

$$\langle \Delta \log \mathcal{L} \rangle_{\text{SM}} = \left\langle \log \left[\left(\frac{\sigma_1}{\sigma_{\{\kappa_i\}}} \right) \left(\frac{d\sigma_{\{\kappa_i\}}}{d\mathbf{x}} \middle/ \frac{d\sigma_1}{d\mathbf{x}} \right) \right] \right\rangle_{\text{SM}}. \qquad (67)$$

We determine this quantity for the pure operator couplings $\mathcal{O}_2$, $\mathcal{O}_3$, $\mathcal{O}_5$, and $\mathcal{O}_6$; the results are shown in Table V. We use only events with $M_{4\ell} = M_X = 125$ GeV (the off-shell cross section is of course small for the SM in any case), hence $\langle \Delta \log \mathcal{L} \rangle_{\text{SM}}$ is 0 for $\mathcal{O}_4$, as this operator is identical to the SM $\mathcal{O}_1$ operator when $M_{4\ell} = M_X$.

In the limit of large statistics, twice the log likelihood ratio is equivalent to the difference in the χ^2 values of the two hypotheses fit to data. Thus, e.g. $3^2/(2\langle \Delta \log \mathcal{L} \rangle_{\text{SM}})$ gives an approximation, valid in the limit of sufficient events, for the expected number of events required to obtain a 3σ limit on the given pure couplings, assuming the tree-level SM is the true theory. This number will undershoot the true value, as we are taking into account neither the irreducible SM background nor detector effects. However, the result is reasonable. The CMS analysis was able to rule out a pure $\mathcal{O}_3$ coupling at slightly greater than 3σ and $\mathcal{O}_2$ at slightly less than 2σ with ~ 20 signal events [61]. This suggests that the number of events needed to obtain a given sensitivity in Table V is smaller than the number of events actually needed in an experiment by a factor of 2–5. (ATLAS reported a slightly less than 3σ exclusion of $\mathcal{O}_3$ in Ref. [63]; they did not report a limit on $\mathcal{O}_2$.)

We note that the $\mathcal{O}_5$ operator, as expected, is harder to distinguish from the SM than the $\mathcal{O}_2$ or $\mathcal{O}_3$ operators. This justifies the postponement of the measurement of this operator, as was suggested in Ref. [45]. Assuming the scaling between the theoretical optimum value in Table V and the actual number of events needed by an experiment for a given sensitivity holds, then 100–200 fb^{-1} of 13 TeV running at LHC should conclusively rule out a pure $\mathcal{O}_5$ coupling, if the Higgs boson is truly SM-like.

TABLE V.   This table gives twice the difference between the average log likelihood obtained assuming pure couplings and the average log likelihood obtained assuming SM ($\mathcal{O}_1$) as evaluated for events generated under the SM ($\mathcal{O}_1$) hypothesis. This value is then used to provide an optimistic estimate of the number of events required for a 3σ exclusion of the specified coupling.

	$\mathcal{O}_1$	$\mathcal{O}_2$	$\mathcal{O}_3$	$\mathcal{O}_4$	$\mathcal{O}_5$	$\mathcal{O}_6$
$2\langle \Delta \log \mathcal{L} \rangle_{\mathrm{SM}}$	0	−0.747	−1.017	0	−0.178	−0.503
Events for 3σ limit	$\cdots$	12.0	8.85	$\cdots$	50.5	17.9

VI. CONCLUSIONS

In this paper we have extended the framework for XZZ coupling measurements in the four-lepton final state presented in Ref. [45] in two important ways: (i) in considering all five operators with dimension ≤ 5, and (ii) in pointing out the effectiveness of the off-shell Higgs boson cross section for determining the coupling structure.

We found that all non-SM operators lead to larger off-shell $gg \to X \to ZZ^* \to 4\ell$ cross sections. This will allow a complementary constraint on (or measurement of) the non-SM couplings of the putative Higgs boson to Z bosons. This is especially true for the $\mathcal{O}_4$ operator; however, its amplitude violates unitarity at relatively low energies (in a way that was quantified above).

Another way to interpret this result is to note that if experimental tests of the invisible Higgs boson width in this channel, along the lines suggested in Refs. [30,49,56,67–69], observe an excess in high invariant mass four-lepton events, then we will be presented with the challenge of determining whether this signal results from the invisible width of the Higgs boson or from higher-dimensional operators, as both serve to enhance the off-shell Higgs boson cross section for a given on-shell Higgs boson cross section. In fact, one could consider the parameter space consisting of the coupling constants for the five operators, κ_{1-5}, and the invisible width of the Higgs. Limits on non-SM XZZ couplings from the Higgs contribution to the off-shell four-lepton cross section are strengthened by the addition of non-negligible invisible width for the Higgs.

We also noted that the "contact operator" $\mathcal{O}_5$ produces very off-shell Z bosons at large $\sqrt{\hat{s}}$. While the cross section for the production of these events is rather small at the LHC, future colliders may be able to measure or constrain κ_5 using this interesting effect.

Future work will include the effect of interference with the $gg \to ZZ$ background explicitly, as this is the dominant effect in constraining the magnitude of Higgs contributions to the four-lepton cross section at large invariant mass. It is particularly interesting to see how the magnitude of this interference changes when varying the XZZ tensor structure. Also of interest is the effect on precision electroweak observables [75,85,88,115] from the five operators considered above, as well as the natural extension to other Higgs boson production processes such as weak vector boson fusion or associated production. We note that while the "golden" four-lepton channel has many benefits, the framework provided here could be easily extended to other channels—in particular, other channels which also involve $X \to VV$ decays.

[1] G. Aad *et al.* (ATLAS Collaboration), Phys. Lett. B **716**, 1 (2012).

[2] S. Chatrchyan *et al.* (CMS Collaboration), Phys. Lett. B **716**, 30 (2012).

[3] J. R. Dell'Aquila and C. A. Nelson, Phys. Rev. D **33**, 80 (1986).

[4] C. A. Nelson, Phys. Rev. D **37**, 1220 (1988).

[5] B. A. Kniehl, Phys. Lett. B **244**, 537 (1990).

[6] A. Soni and R. M. Xu, Phys. Rev. D **48**, 5259 (1993).

[7] D. Chang, W.-Y. Keung, and I. Phillips, Phys. Rev. D **48**, 3225 (1993).

[8] V. D. Barger, K.-m. Cheung, A. Djouadi, B. A. Kniehl, and P. M. Zerwas, Phys. Rev. D **49**, 79 (1994).

[9] T. Arens and L. M. Sehgal, Z. Phys. C **66**, 89 (1995).

[10] S. Y. Choi, D. J. Miller, M. M. Muhlleitner, and P. M. Zerwas, Phys. Lett. B **553**, 61 (2003).

[11] B. C. Allanach, K. Odagiri, M. J. Palmer, M. A. Parker, A. Sabetfakhri, and B. R. Webber, J. High Energy Phys. 12 (2002) 039.

[12] C. P. Buszello, I. Fleck, P. Marquard, and J. J. van der Bij, Eur. Phys. J. C **32**, 209 (2004).

[13] S. Schalla, Report No. IEKP-KA-2004-14.

[14] R. M. Godbole, D. J. Miller, and M. M. Muhlleitner, J. High Energy Phys. 12 (2007) 031.

[15] V. A. Kovalchuk, J. Exp. Theor. Phys. **107**, 774 (2008).

[16] W.-Y. Keung, I. Low, and J. Shu, Phys. Rev. Lett. **101**, 091802 (2008).

[17] O. Antipin and A. Soni, J. High Energy Phys. 10 (2008) 018.

[18] Q.-H. Cao, C. B. Jackson, W.-Y. Keung, I. Low, and J. Shu, Phys. Rev. D **81**, 015010 (2010).

[19] Y. Gao, A. V. Gritsan, Z. Guo, K. Melnikov, M. Schulze, and N. V. Tran, Phys. Rev. D **81**, 075022 (2010).

[20] A. De Rujula, J. Lykken, M. Pierini, C. Rogan, and M. Spiropulu, Phys. Rev. D **82**, 013003 (2010).

[21] C. Englert, C. Hackstein, and M. Spannowsky, Phys. Rev. D **82**, 114024 (2010).

[22] A. Matsuzaki and H. Tanaka, arXiv:1101.2104.

[23] U. De Sanctis, M. Fabbrichesi, and A. Tonero, Phys. Rev. D **84**, 015013 (2011).

[24] H. E. Logan and J. Z. Salvail, Phys. Rev. D **84**, 073001 (2011).

[25] J. S. Gainer, K. Kumar, I. Low, and R. Vega-Morales, J. High Energy Phys. 11 (2011) 027.

[26] I. Low, P. Schwaller, G. Shaughnessy, and C. E. M. Wagner, Phys. Rev. D **85**, 015009 (2012).

[27] C. Englert, M. Spannowsky, and M. Takeuchi, J. High Energy Phys. 06 (2012) 108.

[28] J. M. Campbell, W. T. Giele, and C. Williams, J. High Energy Phys. 11 (2012) 043.

[29] J. M. Campbell, W. T. Giele, and C. Williams, arXiv:1205.3434.

[30] N. Kauer and G. Passarino, J. High Energy Phys. 08 (2012) 116.

[31] B. A. Kniehl and O. L. Veretin, Phys. Rev. D **86**, 053007 (2012).

[32] J. W. Moffat, arXiv:1207.6015.

[33] B. Coleppa, K. Kumar, and H. E. Logan, Phys. Rev. D **86**, 075022 (2012).

[34] S. Bolognesi, Y. Gao, A. V. Gritsan, K. Melnikov, M. Schulze, N. V. Tran, and A. Whitbeck, Phys. Rev. D **86**, 095031 (2012).

[35] R. Boughezal, T. J. LeCompte, and F. Petriello, arXiv:1208.4311.

[36] D. Stolarski and R. Vega-Morales, Phys. Rev. D **86**, 117504 (2012).

[37] P. Cea, arXiv:1209.3106.

[38] J. Kumar, A. Rajaraman, and D. Yaylali, Phys. Rev. D **86**, 115019 (2012).

[39] C.-Q. Geng, D. Huang, Y. Tang, and Y.-L. Wu, Phys. Lett. B **719**, 164 (2013).

[40] P. Avery, D. Bourilkov, M. Chen, T. Cheng, A. Drozdetskiy, J. S. Gainer, A. Korytov, K. T. Matchev et al., Phys. Rev. D **87**, 055006 (2013).

[41] E. Masso and V. Sanz, Phys. Rev. D **87**, 033001 (2013).

[42] Y. Chen, N. Tran, and R. Vega-Morales, J. High Energy Phys. 01 (2013) 182.

[43] A. Menon, T. Modak, D. Sahoo, R. Sinha, and H.-Y. Cheng, Phys. Rev. D **89**, 095021 (2014).

[44] S. Kanemura, M. Kikuchi, and K. Yagyu, Phys. Rev. D **88**, 015020 (2013).

[45] J. S. Gainer, J. Lykken, K. T. Matchev, S. Mrenna, and M. Park, Phys. Rev. Lett. **111**, 041801 (2013).

[46] G. Isidori, A. V. Manohar, and M. Trott, Phys. Lett. B **728C**, 131 (2014).

[47] J. Frank, M. Rauch, and D. Zeppenfeld, Eur. Phys. J. C **74**, 2918 (2014).

[48] B. Grinstein, C. W. Murphy, and D. Pirtskhalava, J. High Energy Phys. 10 (2013) 077.

[49] F. Caola and K. Melnikov, Phys. Rev. D **88**, 054024 (2013).

[50] S. Banerjee, S. Mukhopadhyay, and B. Mukhopadhyaya, Phys. Rev. D **89**, 053010 (2014).

[51] Y. Sun, X.-F. Wang, and D.-N. Gao, Int. J. Mod. Phys. A **29**, 1450086 (2014).

[52] I. Anderson, S. Bolognesi, F. Caola, Y. Gao, A. V. Gritsan, C. B. Martin, K. Melnikov, M. Schulze et al., Phys. Rev. D **89**, 035007 (2014).

[53] M. Chen, T. Cheng, J. S. Gainer, A. Korytov, K. T. Matchev, P. Milenovic, G. Mitselmakher, M. Park, A. Rinkevicius, and M. Snowball, Phys. Rev. D **89**, 034002 (2014).

[54] G. Buchalla, O. Cata, and G. D'Ambrosio, Eur. Phys. J. C **74**, 2798 (2014).

[55] Y. Chen and R. Vega-Morales, J. High Energy Phys. 04 (2014) 057.

[56] J. M. Campbell, R. K. Ellis, and C. Williams, J. High Energy Phys. 04 (2014) 060.

[57] Y. Chen, E. Di Marco, J. Lykken, M. Spiropulu, R. Vega-Morales, and S. Xie, arXiv:1401.2077.

[58] M. Gonzalez-Alonso and G. Isidori, Phys. Lett. B **733**, 359 (2014).

[59] S. Chatrchyan et al. (CMS Collaboration), Phys. Rev. Lett. **110**, 081803 (2013).

[60] G. Aad et al. (ATLAS Collaboration), Phys. Lett. B **726**, 120 (2013).

[61] S. Chatrchyan et al. (CMS Collaboration), Phys. Rev. D **89**, 092007 (2014).

[62] CMS Collaboration, Report No. CMS-PAS-HIG-12-041.

[63] ATLAS Collaboration, Report No. ATLAS-CONF-2013-013.

[64] CMS Collaboration, Report No. CMS-PAS-HIG-13-002.

[65] ATLAS Collaboration, Report No. ATLAS-CONF-2013-040.

[66] CMS Collaboration, Report No. CMS-PAS-HIG-13-005.

[67] N. Kauer, Mod. Phys. Lett. A **28**, 1330015 (2013).

[68] J. M. Campbell, R. K. Ellis, and C. Williams, Phys. Rev. D **89**, 053011 (2014).

[69] G. Passarino, Eur. Phys. J. C **74**, 2866 (2014).

[70] S. Dawson, A. Gritsan, H. Logan, J. Qian, C. Tully, R. Van Kooten, A. Ajaib, A. Anastassov *et al.*, arXiv:1310.8361.

[71] R. Contino, M. Ghezzi, C. Grojean, M. Muhlleitner, and M. Spira, J. High Energy Phys. 07 (2013) 035.

[72] P. Artoisenet, P. de Aquino, F. Demartin, R. Frederix, S. Frixione, F. Maltoni, M. K. Mandal, P. Mathews *et al.*, J. High Energy Phys. 11 (2013) 043.

[73] F. Boudjema, G. Cacciapaglia, K. Cranmer, G. Dissertori, A. Deandrea, G. Drieu la Rochelle, B. Dumont, U. Ellwanger *et al.*, arXiv:1307.5865.

[74] A. Alloul, B. Fuks, and V. Sanz, J. High Energy Phys. 04 (2014) 110.

[75] I. Brivio, T. Corbett, O. J. P. Éboli, M. B. Gavela, J. Gonzalez-Fraile, M. C. Gonzalez-Garcia, L. Merlo, and S. Rigolin, J. High Energy Phys. 03 (2014) 024.

[76] R. Contino, M. Ghezzi, C. Grojean, M. Muhlleitner, and M. Spira, Comput. Phys. Commun. **185**, 3412 (2014).

[77] S. Banerjee, S. Mukhopadhyay, and B. Mukhopadhyaya, J. High Energy Phys. 10 (2012) 062.

[78] G. F. Giudice, P. Paradisi, A. Strumia, and A. Strumia, J. High Energy Phys. 10 (2012) 186.

[79] M. Baak, M. Goebel, J. Haller, A. Hoecker, D. Kennedy, R. Kogler, K. Moenig, M. Schott, and J. Stelzer, Eur. Phys. J. C **72**, 2205 (2012).

[80] B. Batell, S. Gori, and L. T. Wang, J. High Energy Phys. 01 (2013) 139.

[81] W. F. Chang, W. P. Pan, and F. Xu, Phys. Rev. D **88**, 033004 (2013).

[82] H. Mebane, N. Greiner, C. Zhang, and S. Willenbrock, Phys. Lett. B **724**, 259 (2013).

[83] A. Hayreter and G. Valencia, Phys. Rev. D **88**, 034033 (2013).

[84] H. Mebane, N. Greiner, C. Zhang, and S. Willenbrock, Phys. Rev. D **88**, 015028 (2013).

[85] S. Gori and I. Low, J. High Energy Phys. 09 (2013) 151.

[86] A. Pich, I. Rosell, and J. J. Sanz-Cillero, J. High Energy Phys. 01 (2014) 157.

[87] M. Baak, A. Blondel, A. Bodek, R. Caputo, T. Corbett, C. Degrande, O. Eboli, J. Erler *et al.*, arXiv:1310.6708.

[88] C.-Y. Chen, S. Dawson, and C. Zhang, Phys. Rev. D **89**, 015016 (2014).

[89] J. Elias-Mir, C. Grojean, R. S. Gupta, and D. Marzocca, J. High Energy Phys. 05 (2014) 019.

[90] K. Cheung, J. S. Lee, E. Senaha, and P. Y. Tseng, J. High Energy Phys. 06 (2014) 149.

[91] R. Nagai, M. Tanabashi, and K. Tsumura, arXiv:1409.1709 [Phys. Rev. D (to be published)].

[92] W. Buchmuller and D. Wyler, Nucl. Phys. **B268**, 621 (1986).

[93] K. Hagiwara, R. D. Peccei, D. Zeppenfeld, and K. Hikasa, Nucl. Phys. **B282**, 253 (1987).

[94] G. F. Giudice, C. Grojean, A. Pomarol, and R. Rattazzi, J. High Energy Phys. 06 (2007) 045.

[95] B. Grzadkowski, M. Iskrzynski, M. Misiak, and J. Rosiek, J. High Energy Phys. 10 (2010) 085.

[96] F. Bonnet, M. B. Gavela, T. Ota, and W. Winter, Phys. Rev. D **85**, 035016 (2012).

[97] T. Corbett, O. J. P. Eboli, J. Gonzalez-Fraile, and M. C. Gonzalez-Garcia, Phys. Rev. D **86**, 075013 (2012).

[98] J. Ellis and T. You, J. High Energy Phys. 09 (2012) 123.

[99] G. Cacciapaglia, A. Deandrea, G. D. La Rochelle, and J. B. Flament, J. High Energy Phys. 03 (2013) 029.

[100] G. Belanger, B. Dumont, U. Ellwanger, J. F. Gunion, and S. Kraml, J. High Energy Phys. 02 (2013) 053.

[101] T. Corbett, O. J. P. Eboli, J. Gonzalez-Fraile, and M. C. Gonzalez-Garcia, Phys. Rev. D **87**, 015022 (2013).

[102] C. Grojean, E. E. Jenkins, A. V. Manohar, and M. Trott, J. High Energy Phys. 04 (2013) 016.

[103] K. Cheung, J. S. Lee, and P. Y. Tseng, J. High Energy Phys. 05 (2013) 134.

[104] J. Elias-Mir, J. R. Espinosa, E. Masso, and A. Pomarol, J. High Energy Phys. 08 (2013) 033.

[105] A. Falkowski, F. Riva, and A. Urbano, J. High Energy Phys. 11 (2013) 111.

[106] P. P. Giardino, K. Kannike, I. Masina, M. Raidal, and A. Strumia, J. High Energy Phys. 05 (2014) 046.

[107] J. Ellis and T. You, J. High Energy Phys. 06 (2013) 103.

[108] A. Djouadi and G. Moreau, Eur. Phys. J. C **73**, 2512 (2013).

[109] T. Corbett, O. J. P. Eboli, J. Gonzalez-Fraile, and M. C. Gonzalez-Garcia, Phys. Rev. Lett. **111**, 011801 (2013).

[110] B. Dumont, S. Fichet, and G. von Gersdorff, J. High Energy Phys. 07 (2013) 065.

[111] P. Bechtle, S. Heinemeyer, O. Stl, T. Stefaniak, and G. Weiglein, Eur. Phys. J. C **74**, 2711 (2014).

[112] G. Belanger, B. Dumont, U. Ellwanger, J. F. Gunion, and S. Kraml, Phys. Rev. D **88**, 075008 (2013).

[113] S. Choi, S. Jung, and P. Ko, J. High Energy Phys. 10 (2013) 225.

[114] J. Elias-Miro, J. R. Espinosa, E. Masso, and A. Pomarol, J. High Energy Phys. 11 (2013) 066.

[115] A. Pomarol and F. Riva, J. High Energy Phys. 01 (2014) 151.

[116] E. Boos, V. Bunichev, M. Dubinin, and Y. Kurihara, Phys. Rev. D **89**, 035001 (2014).

[117] R. L. Delgado, A. Dobado, and F. J. Llanes-Estrada, J. High Energy Phys. 02 (2014) 121.

[118] S. Willenbrock and C. Zhang, arXiv:1401.0470.

[119] C. Englert, A. Freitas, M. M. Mhlleitner, T. Plehn, M. Rauch, M. Spira, and K. Walz, J. Phys. G **41**, 113001 (2014).

[120] J. Ellis, V. Sanz, and T. You, J. High Energy Phys. 07 (2014) 036.

[121] C. Englert and M. Spannowsky, Phys. Rev. D **90**, 053003 (2014).

[122] E. Masso, J. High Energy Phys. 10 (2014) 128.

[123] J. de Blas, M. Ciuchini, E. Franco, D. Ghosh, S. Mishima, M. Pierini, L. Reina, and L. Silvestrini, arXiv:1410.4204.

[124] C. Englert, Y. Soreq, and M. Spannowsky, arXiv:1410.5440.

[125] J. Ellis, V. Sanz, and T. You, arXiv:1410.7703.

[126] A. Bredenstein, A. Denner, S. Dittmaier, and M. M. Weber, Phys. Rev. D **74**, 013004 (2006).

[127] A. Bredenstein, A. Denner, S. Dittmaier, and M. M. Weber, J. High Energy Phys. 02 (2007) 080.

[128] K. Kondo, J. Phys. Soc. Jpn. **57**, 4126 (1988).

[129] K. Kondo, J. Phys. Soc. Jpn. **60**, 836 (1991).

[130] K. Kondo, T. Chikamatsu, and S. H. Kim, J. Phys. Soc. Jpn. **62**, 1177 (1993).

[131] R. H. Dalitz and G. R. Goldstein, Phys. Rev. D **45**, 1531 (1992).

[132] B. Abbott *et al.* (D0 Collaboration), Phys. Rev. D **60**, 052001 (1999).

[133] J. C. Estrada Vigil, Report No. FERMILAB-THESIS-2001-07.

[134] M. F. Canelli, Report No. UMI-31-14921.

[135] V. M. Abazov *et al.* (D0 Collaboration), Nature (London) **429**, 638 (2004).

[136] J. S. Gainer, J. Lykken, K. T. Matchev, S. Mrenna, and M. Park, arXiv:1307.3546.

[137] J. Alwall, M. Herquet, F. Maltoni, O. Mattelaer, and T. Stelzer, J. High Energy Phys. 06 (2011) 128.

[138] A. Belyaev, N. D. Christensen, and A. Pukhov, Comput. Phys. Commun. **184**, 1729 (2013).

[139] A. Alloul, N. D. Christensen, C. Degrande, C. Duhr, and B. Fuks, Comput. Phys. Commun. **185**, 2250 (2014).

[140] E. W. N. Glover and J. J. van der Bij, Nucl. Phys. **B321**, 561 (1989).

[141] T. Matsuura and J. J. van der Bij, Z. Phys. C **51**, 259 (1991).

[142] C. Zecher, T. Matsuura, and J. J. van der Bij, Z. Phys. C **64**, 219 (1994).

[143] Z. Bern, L. J. Dixon, and D. A. Kosower, Nucl. Phys. **B513**, 3 (1998).

[144] T. Binoth, M. Ciccolini, N. Kauer, and M. Kramer, J. High Energy Phys. 03 (2005) 065.

[145] C. Anastasiou, G. Dissertori, and F. Stckli, J. High Energy Phys. 09 (2007) 018.

[146] M. Grazzini, J. High Energy Phys. 02 (2008) 043.

[147] T. Binoth, N. Kauer, and P. Mertsch, arXiv:0807.0024.

[148] J. M. Campbell, R. K. Ellis, and C. Williams, J. High Energy Phys. 07 (2011) 018.

[149] J. F. Gunion, H. E. Haber, G. L. Kane, and S. Dawson, *The Higgs Hunter's Guide*, Frontiers in Physics (Westview Press, Cambridge, 2000).

[150] A. Djouadi, Phys. Rep. **457**, 1 (2008).

[151] B. W. Lee, C. Quigg, and H. B. Thacker, Phys. Rev. D **16**, 1519 (1977).

[152] A. Dobado, M. J. Herrero, J. R. Pelaez, and E. Ruiz Morales, Phys. Rev. D **62**, 055011 (2000).

[153] M. Dahiya, S. Dutta, and R. Islam, arXiv:1311.4523.

[154] S. Chatrchyan *et al.* (CMS Collaboration), J. High Energy Phys. 01 (2013) 063.

[155] Patricia Rebello Teles (CMS Collaboration), arXiv:1310.0473.

[156] J. Neyman and E. S. Pearson, Phil. Trans. R. Soc. A **231**, 289 (1933).